Proceedings of HT-FED04
2004 ASME Heat Transfer/Fluids Engineering Summer Conference
July 11-15, 2004, Charlotte, North Carolina USA

HT-FED04-56653

Nano-PTV using Confocal Microscopy

Jae S. Park, Chang K. Choi and Kenneth D. Kihm[1]
Micro/Nano-scale Fluidics and Heat Transport Laboratory
Department of Mechanical Engineering, Texas A&M University, College Station, TX 77843
(http://go.to/microlab)

ABSTRACT

A conventional microscopy and confocal microscopy was used to enable nano-particle tracking using a three-dimensional (3-D) diffraction image pattern caused by an optical aberration. The Point Spread Function (PSF) of a particle image is known as a function of a defocus distance from a focal plane. Using the PSF of nano-particles, particle's x and y positions as well as z-position can be obtained. A dry objective lens (40X, 0.75NA) is used to detect diffraction patterns of 500-nm fluorescent micro-spheres suspended in water solution inside a 100-μm square micro-tube. The purposes of this presented study are to investigate experimentally the 3-D PSF of fluorescent nano-particle in thick specimen and to develop the 3-D particle tracking technique using 3-D diffraction images of conventional microscopy and CLSM.

NOMENCLATURE

a	Radius of the objective aperture
f	Focal length
M	Magnification
n	Refractive index
NA	Numerical aperture
J_0	Bessel function of zero-order
t	Thickness of glass
u	Longitudinal non-dimensional variable
v	Transversal non-dimensional variable
ρ	Radial variable perpendicular to the axis
Δz	Defocus distance

1. INTRODUCTION

In mechanical engineering, the fluorescence microscopy system has been applied to fluid mechanics at a micron level. A particle imaging velocimetry using a fluorescence microscopy has developed successfully and become a useful technique for measuring a velocity field (Santiago *et al* 1998). By the way, some optical limitations caused by diffraction and optical aberration made the particle imaging system unable to easily observe a variety of microscopic test specimens. The quality of particle image was degraded by such an out-of-focus of particle, a background noise, and a diffraction-limited spot size. A series of theoretical and experimental studies was performed to alleviate the optical difficulties and improve the particle visibility (Olsen and Adrian 2000, Meinhart *et al* 2000, Meinhart and Wereley 2003).

The nano-particle tracking technique basically uses a microscope system utilizing a high-NA objective lens and a microscopic specimen. By the way, the conventional microscope system has a few difficulties caused by diffraction in visualizing the nano particles. The optical diffraction theory has been studied very well for last hundreds years, and has become a fundamental knowledge for many optical studies dealing with a microscopic imaging formation (Born and Wolf 1965). Regarding on the diffraction theory, a number of optical instruments and techniques have been developed to get good image information through a video microscopy system (Inoué and Spring 1997). One of the innovative developments has been the CLSM, which has an optically sliced image thickness of sub-micron resolution and can build a 3-D image by scanning a focused beam through a 3-D specimen point by point (Webb 1996, Wilson 1990).

Richards and Wolf (1959) found the 3-D amplitude PSF for an objective in a uniform medium by using an electromagnetic wave falling on a hole as a source for the field at any point. After Born and Wolf (1965) made a comprehensive synthesis of diffraction theory, a lot of writers have discussed theoretically and experimentally the 3-D diffraction patterns and the effects of aberration. Gibson and Lanni (1991) considered a practical object structure that consisted of an oil-immersion layer, a cover glass and a specimen layer. They computed many aberrated PSFs produced by the practical specimen of an oil-immersion lens using a modified Kirchhoff's diffraction formula. In addition, a water-immersion objective system was tested theoretically by the computed PSFs based on the Gibson and Lanni's equation,

[1] Corresponding author

and the obtained PSF was compared with the data acquired with an oil-immersion lens system (Kontoyannis and Lanni 1996). McNally *et al* (1994) applied the Gibson and Lanni's equation to a dry objective system, and measured PSFs of 260-nm fluorescences microsphere by using a computational optical sectioning microscopy.

The effects of aberrations in CLSM were also studied by Sheppard (1988), who considered an appropriate form for the aberration function for an optical system of high numerical aperture. The 3-D intensity distribution for confocal system was based on Huygens-Fresnel principle and the aberration fuction is expanded in a series of spherical harmonics with an associated Legendre function (Sheppard 1988). A spherical aberration is introduced normally when an objective lens is focusing deep within the thick specimen. Sheppard and Gu (1991) studied how to compensate the aberration in CLSM. They considered two kinds of compensation ways: an immersing a dielectric slab into a lens system and an altering the effective tube length of microscope. The axial response intensities were calculated for the case of imaging through a slab and for a change of tube length.

A nano-particle tracking technique using a 3-D PSF has already become a useful method in a biological science. Kao and Verkman (1994) achieved a 3-D high-precision tracking of single fluorescent particle by using a modified fluorescence microscope containing a cylindrical lens between a detector and an objective lens. They encoded 3-D positional information using the image shape and orientation with a lateral resolution of 5 nm and an axial resolution of 12 nm every 0.54s. Speidel *et al* (2003) recently performed another 3-D tracking of fluorescence particle using off-focus imaging with sub-nanometer precision. The seeding particles embedded in specimen at different distance from focal plane presented the full 3-D diffraction patterns and were precisely encoded by the number and diameter of rings, relative intensity of rings.

2. Theory

2.1 Diffraction and Point Spread Function (PSF)

The diffraction, in general, occurs because a large number of light waves emitted from the point source and passing through a rear aperture of objective lens are superposed constructively or destructively by phase differences of waves. When a source point in specimen is observed using an optical microscope, the image is formed as a 2-D Airy diffraction pattern having a transversely spread in the image plane. It is a role of the objective lens to focus the waves into an infinitely small point for a perfect image formation, but the waves interfere with each other near the focal point to produce the diffraction pattern. The off-focused source point in the specimen, as a rule, is represented by a much widely spread diffraction pattern rather than the well-focused source point. In figure 1, the diffraction pattern is produced differently as long as the source point is focused well or not, so it can be expressed in terms of a defocus distance (Δz) and x and y positions in the image plane. The defocus denotes a distance between a source point and a focal plane of lens.

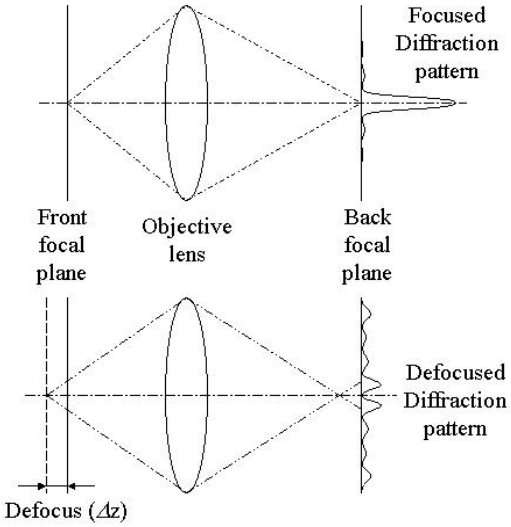

Figure 1. Illustration of the diffraction in microscopy system

The 3-D diffraction pattern is called as a point spread function (PSF) that is generated from stacks of serial optical sections. The PSF can be expressed with a xyz coordinate in the image plane, and is extended periodically and symmetrically above and below a focal plane along the optical axis as well as radially around the axis. A monochromatic spherical wave emitted from the point source transverse an entrance pupil of an objective lens and emerges from an exit pupil of the objective lens, and converges towards the back focal point O. The PSF, $U(u,v)$, at a typical point P in the neighborhood of O can be predicted on a basis of the principle of interference is called the *Huygens-Fresnel Principle*. In consequence, the PSF is expressed with convergent series of Bessel function and exponential terms as shown in equation (1) (Born and Wolf 1965, p 437).

$$h(u,v) = -\frac{2\pi\, i\, a^2 A}{\lambda f^2} e^{i\left(\frac{f}{a}\right)^2 u} \int_0^1 e^{-\frac{1}{2} i u \rho^2} J_0(v\rho)\rho\, d\rho \qquad (1)$$

where $u = \frac{2\pi}{\lambda}\left(\frac{a}{f}\right)^2 z$ and $v = \frac{2\pi}{\lambda}\left(\frac{a}{f}\right) r = \frac{2\pi}{\lambda}\frac{a}{f}\sqrt{x^2+y^2}$.

The u and v are longitudinal and transversal non-dimensional variables of a cylindrical coordinate in the image plane. Note that the Bessel function term is a function of only v variable, and the exponential term is a function of only u variable. This means that the axial and lateral diffraction

patterns of a PSF are respectively produced in terms of the exponential function and the Bessel function.

Now, we need to find an intensity distribution of an image, which is identical with an actual information obtained by the detector, and in case of the conventional microscopy system, it is calculated by $I(u,v) = |h(u,v)|^2$.

2.2 Aberration in the imaging formation

Aberration is that light rays emerged from several radial points of a lens are not converged into one focal point but focused on different points on the axis. Owing to the aberration of the microscope objectives a specimen image appears blurred and slightly out of focus. Ideally, an aberration-free microscopy system makes all light waves refracted by the lens direct to an exact focal point in the center of the image plane to produce a perfect image. Generally, the aberration-free microscopy produces a symmetric diffraction pattern along the optical axis, but some optical aberrations affect the diffraction image to be asymmetric above and below an exact focus, and the PSF becomes distorted and displaced along the optical axis of microscope.

A conventional microscopy system has a flat specimen and observes close to a cover slip. The light ray from the observation point passes through the cover slip and the immersion medium having the ideal conditions of thickness and refractive index, and then travels to the detector located on exact image plane. This is called as an aberration-free or a designed system. Under non-designed system, some of aberrations are commonly caused by the failure to maintain the designated optical tube length or the using of substances (cover slip) and immersion medium having false refractive index and thickness. Figure 2 illustrates the aberration-free system of designed conditions and the aberrated system of non-designed conditions. The designed conditions in aberration-free system depend on the objective lens, which is specified with a cover slip of designated refractive index (n_{g*}) and thickness (t_{g*}), and an immersion medium of designated refractive index (n_{i*}) and thickness (t_{i*}). The thickness (t_{s*}) of specimen should be zero in the designed system. The optical tube length is measured from the back focal plane of the objective lens to the image plane, and is usually around 160 mm for conventional microscopes.

The most main causes of aberrations are the presence of thick specimen and the mismatching of refractive indices. As shown in figure 2, the source point in the designed system is located immediately below the cover slip, but the observation point of the non-designed system may be located deeply in the specimen. The aqueous medium of a specimen, in general, has a different refractive index from those of a cover slip and an immersion medium, and the light rays are refracted at two interfaces between three different mediums. The refracted rays have optical pathways transformed from the original aberration-free condition and do not converge to the original focal point. In consequence, the refraction by the index mismatching affects the optical aberration of an objective lens and produces an asymmetric diffraction pattern in the image plane. By the way, if the refractive index of specimen matches to that of immersion medium, any thickness of specimen approximately meets the design condition (Gibson and Lanni 1991).

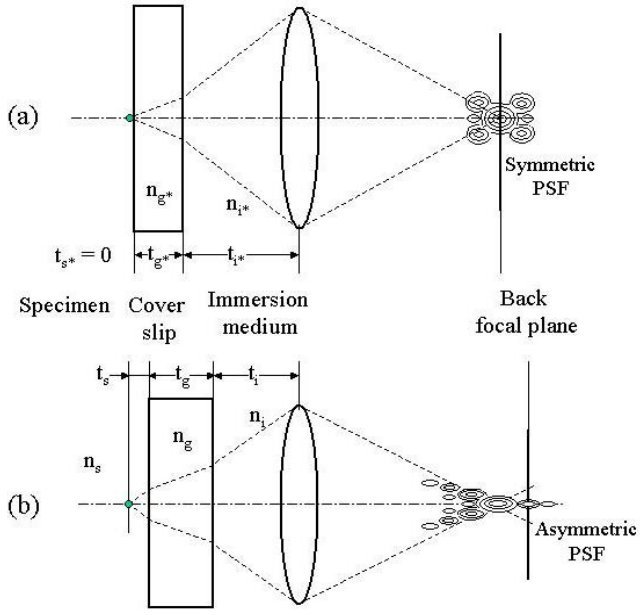

Figure 2. Illustrations of (a) aberration-free system and (b) aberrated system

2.3 Theoretical models of PSF in CLSM

The PSF of CLSM is derived from the coherent optical imaging formation in scanning microscopes using a detector, the area of which is limited by a pinhole (Wilson 1990). In a reflection CLSM, the light illuminated from the laser is focused by the objective into a specimen, and the reflected light is refocused onto a detector in the image plane by the collector, which is physically the same as the objective lens. Before the reflected lights emerged the specimen converges on the detector, the pinhole let only an exactly focused light ray pass through but the off-focused lights are blocked. The two PSFs of excitation and emission lights are considered to produce a confocal PSF.

The PSF of the excitation light, $h_{ex}(u,v)$, is given by the Hankel transform of the pupil function:

$$h_{ex}(u,v) = 2\int_0^{\infty} P_{ex}(\rho)\, e^{\frac{1}{2}iu\rho^2} J_0(v\rho)\rho\, d\rho\,. \qquad (2)$$

The PSF of the emission light, $h_{em}(u,v)$, is given by:

$$h_{em}(u,v) = 2\int_0^{\infty} P_{em}(\rho)\, e^{\frac{1}{2}iu\rho^2} J_0(v\rho)\rho\, d\rho\,. \qquad (3)$$

In the above equation, $\rho = r/a_1$, where r is the actual radial co-ordinate and a_1 is the radius of the pupil, $v = kr(\sin\alpha_1)$, where k is the wave number ($= 2\pi/\lambda$), λ is the wavelength, and α_1 is the angular aperture of the objective, $u = 4kz(\sin^2(\alpha_1/2))$, and $P(\rho)$ is the pupil function of the objective.

Now, the image formation depends critically on the form of the pupil function, $P(\rho)$. In general, the PSF of Conventional Microscopy having an in-coherent optical system can be expressed by only one of both PSFs:

$$h_{conventional}(u,v) = \left|h(u,v)\right|. \tag{4}$$

However, the CLSM has the form of an effective PSF, which is given by the product of the excitation PSF and the emission PSF, and is expressed by:

$$h_{CLSM}(u,v) = \left|h_{em}(u,v)\,h_{ex}(u,v)\right|. \tag{5}$$

In CLSM, the coherent lights of excitation and emission are employed simultaneously to image the object and the image is built up by scanning the specimen and the detector in synchronism. The characteristic of CLSM makes two PSFs of lights equal, and the PSF of CLSM can be expressed as a product of two PSFs of conventional microscopy.

$$h_{CLSM}(u,v) = \left|h(u,v)\right|^2 = \left[h_{conventional}(u,v)\right]^2 \tag{6}$$

In consequence, the intensity distribution of CLSM can be simply expressed as the product of two intensity distributions of conventional microscopy.

$$I_{CLSM}(u,v) = \left[I_{conventional}(u,v)\right]^2 = \left|h(u,v)\right|^4 \tag{7}$$

From the intensity distribution $I(x_d, y_d, \Delta z)$ based on Gibson and Lanni's equation (1991), the 3-D intensity distribution of CLSM can be expressed as:

$$I(x_d, y_d, \Delta z) = \left| C\int_0^1 J_0\left[k\frac{NA}{\sqrt{M^2 - NA^2}}\rho\sqrt{x_d^2 + y_d^2}\right] exp\left[jW(\Delta z, \rho)\right]\rho\, d\rho \right|^4 . \tag{8}$$

3. Experimental set-up

The presented experiment was performed with two different kinds of fluorescence microscopy systems, which are conventional microscopy and CLSM. The first system, conventional microscopy consists of an upright Olympus BX 61 microscope with a 100-W mercury lamp, a digital CCD camera (UNIQ Vision Inc, UP-1830) equipped with a Sony 2/3" Exview HAD CCD chip (1024×1024 pixels, 6.45-μm pixel width), and a Windows XP computer equipped with a frame grabber (QED-Imaging) which records images as an 8-bit signal with 30 fps. The second, CLSM system's principal components are a YOKOGAWA CSU-10 confocal unit (Solamere Technology Group) and an Ar-ion laser (LaserPhysics) as an illuminating source, and they are additionally equipped to the given conventional microscopy (Park *et al* 2003). The CSU-10 confocal unit is mounted between the BX-61 microscope and the CCD camera of conventional microscopy, and the Ar-ion laser is connected to the CSU-10 confocal unit by using a single-mode optical fiber (OZ optics).

The used seeding particle is a yellow-green (EX 505 / EM 515) fluorescent polystyrene micro-sphere (Molecular Probes), which has a diameter of 0.5-μm and a density of 1.055 g/cm^3. The micro-sphere's diameter is less than halves of the axial resolutions of both conventional microscopy and CLSM. To image the fluorescence beads, two microscopy systems are using a similar epi-fluorescence filter system. In conventional microscopy, a light beam having a specific wavelength is selected from a wide spectrum of wavelengths of the mercury lamp by using an epi-fluorescence filter unit, which is composed with an excitation filter (470 – 490 nm), a dichroic mirror (505 nm) and a barrier filter (510 nm). Each filter and mirror is used to select a specific pumping wavelength for the fluorescent beads, to reflect the pumping wavelength and transmit the fluorescent wavelength, and to filter out other than fluorescent wavelength. In CLSM, the Ar-ion laser emits a continuous wavelength of 488-nm having a power of 50-mW, and an epi-fluorescence filter system is equipped inside CSU-10.

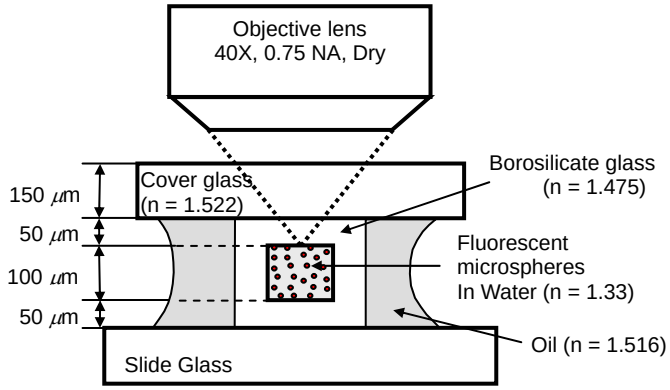

Figure3. Schematic of a micro-channel specimen.

The test specimen was fabricated by using a square micro-channel, which was made out of borosilicate glass (n_c=1.475) and by Vitrocom. In figure 3 the channel's inner-width is 100 μm and the wall thickness is 50 μm. A 0.15-mm thick cover slip was bonded on the micro-channel, and between both parts a micron-scale air layer existed probably. To fill the thin air

layer immersion oil was used and the oil was spread to air-space next to both sides of channel. The combination of cover slip, channel wall and oil operated as a single cover slip having a thickness of 200-μm and a refractive index of 1.515. The sample's non-designed conditions cause an optical aberration in the microscopic imaging formation, and result in an important transformation in resolution and contrast of fluorescence particle image.

4. RESULTS AND DISCUSSION

Figure 4 shows two law particle images captured by a conventional microscopy and CLSM of the experimental test section illustrated in figure 3. The conventional microscopy image shows various diameters of diffraction fringes that should be related with a defocus distance (Δz). The indicated numbers mean the defocus distance from the focal plane which is focused on the top inner glass wall of the square channel. The defocus distances were obtained from the theoretical PSF equation of Gibson and Lanni (1991) which could account for a relation between Δz and the diffraction pattern.

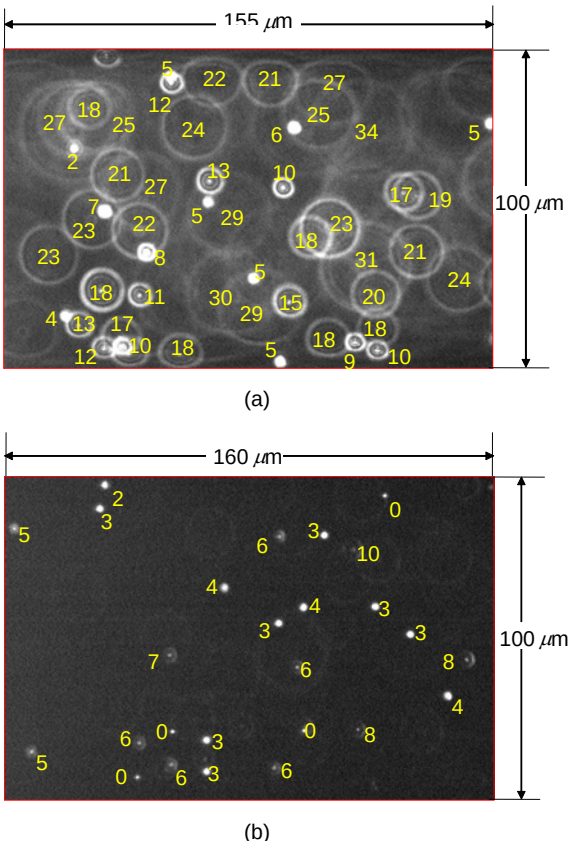

Figure 4. 3-D diffraction image field of 500-nm diameter polystyrene fluorescent particles inside a square micro-channel illustrated in figure 2: (a) conventional microscopy and (b) CLSM.

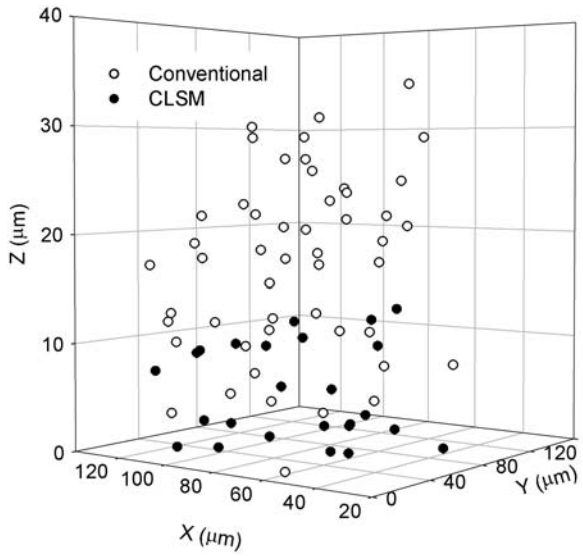

Figure 5. 3-D particle distributions of figure 4's images.

The conventional microscopy shows more particles than CLSM even though both images used same solid volume concentration (0.0004%) of particle solution. The conventional microscopy could not make a spatial filtering that is a typical function of CLSM. That is a reason why the conventional microscopy shows many off-focused images rather than CLSM. Figure 5 shows the particles' xyz positions of both microcopies corresponding to figure 4 (a) and (b). Note that the shallow focal depth of CLSM is caused from its own optical slice thickness. By the way, this study is concentrated on the off-focused diffraction images, which can be used for 3-dimensional tracking.

The presented experiment took the consecutive images of diffraction patterns in both systems, and analyzed the out-most fringe's diameter to get the particle positions at every image. Every particle had changed the out-most fringes' diameters image by image and the changes of diameters mean the movement in z-direction. By means of this z-position tracking, every particle could be tracked three-dimensionally.

Brownian motion of 500-nm particles could be tracked in the isotropic direction using the presented method. First, the x and y position could be known by finding the centers of the diffraction images. Next, the z-positions of particles should be tracked by measuring the out-most fringe diameters. Figure 6 shows the 2-dimensional displacements of Brownian motion of 500-nm particles suspended in water at 22 ^{o}C. The frame rate of images was 30 frames/sec and the capturing time was 1 second. The lateral and axial resolutions of the measurement were 0.16-μm. The six particles, which are arbitrarily chosen to be least 10 micro-meter away from the wall, were used to evaluate Brownian displacement, and the total displacement

samples were 174. In figure 6, three 2-dimensional displacements do not

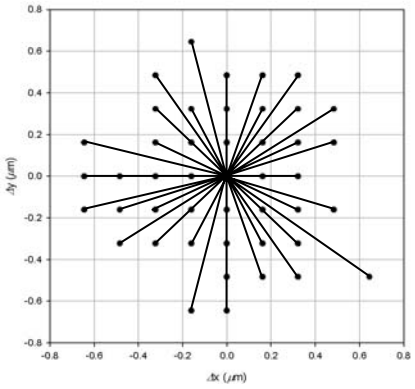

(a) X-Y Plane

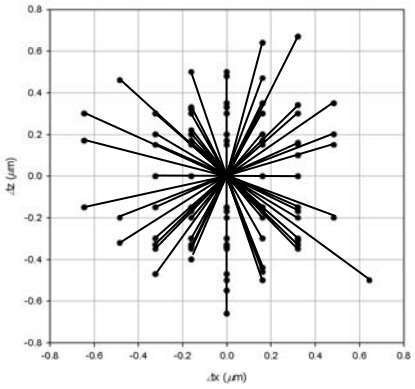

(b) X-Z Plane

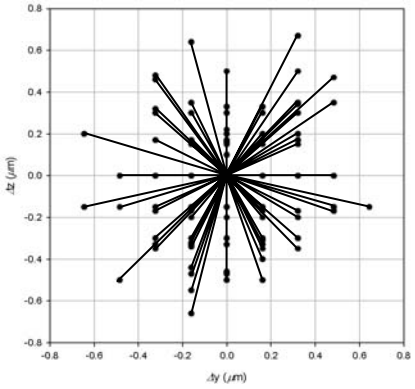

(c) Y-Z Plane

Figure 6. Two-dimensional Brownian displacements.

show anisotropic distributions of Brownian motion. This means that the z-position tracking is much reasonable and adoptable.

In general, Brownian motion can be evaluated by the mean square displacement of the particle, which is expressed as $\langle r^2 \rangle = 6D\Delta t$, where D means a diffusivity (or diffusion coefficient) of single particle and Δt is time interval of each displacement. $6D\Delta t$ is a three-dimensional mean square displacement.

Table1. Comparison of theoretical predictions with measured data for Brownian motion of 500-nm particles in water at 22°C for a time interval of 33-ms

	Mean-Square-Displacement (μm^2)	
Dimension	Theory	Measurement
X	0.059	0.054
Y	0.059	0.058
Z	0.059	0.06
X-Y	0.119	0.113
X-Z	0.119	0.115
Y-Z	0.119	0.119
XYZ	0.178	0.173

Additionally, one and two dimensional mean square displacements are $2D\Delta t$ and $4D\Delta t$, respectively.

Following the well-known Stokes-Einstein equation, the diffusivity is given by

$$D = \frac{\kappa T}{6\pi\mu r_p} \tag{9}$$

where the κ is Boltzmann's constant (1.42×10^{-23} J/K), T is the absolute temperature of the fluid, μ is the dynamic viscosity of the fluid, and r_p is the particle radius. This experiment was performed at 22°C, and r_p was 0.25 μm. So, the diffusion coefficient was about 0.9 $\mu m^2/s$, and the time interval (Δt) was 33 ms. Table 1 shows the theoretical values and experimental data of mean square displacement of Brownian motion. According the table, the experimental data of all dimensions agree to those of theory so well.

CONCLUSION

A conventional microscopy and confocal microscopy were applied to track three-dimensionally nano-particles using PSFs. The 3-D PSFs of 500-nm fluorescent particles were theoretically calculated for an experimental test section, and the corresponding measurements were performed to validate a given theoretical model.

A micro-tube test section having a deep specimen and a mismatched cover glass, which affected an aberration, causes the asymmetric diffraction patterns. Using the theoretical PSF for the non-designed specimen structure, particles' z-direction positions could be obtained from a relation between a defocus distance and PSF.

The nano-particles in a micro-tube could be tracked with a lateral and an axial resolution of 0.16-μm, and a 33-ms time interval. The diffusivity and mean-square-displacement of Brownian particles are obtained from the tracking and do well agree to an Einstein's theory.

ACKNOWLEDGMENTS

The authors are grateful to the financial support sponsored partially by the NASA-Fluid Physics Research Program Grant No. NAG 3-2712, and partially by the US-DOE/Argonne National Laboratory Grant No. DE-FG02-04ER46101. The presented technical contents are not necessarily the representative views of NASA, US-DOE or Argonne National Laboratory.

REFERENCES

Born, M. and Wolf, E., 1965, *Principles of Optics*, Pergamon, New York.

Gibson, F. S. and Lanni, F., 1991, "Experimental test of an analytical model of aberration in an oil-immersion objective lens used in three-dimensional light microscopy," J. Opt. Soc. Am. A, Vol. 8, pp. 1601-1613.

Inoué, S. and Spring, K. R., 1997, *Video Microscopy: The Fundamentals*, Plenum Press, New York, pp 26-65.

Kao, H. P. and Verkman, A. S., 1994, "Tracking of single fluorescent particles in three dimensions: use of cylindrical optics to encode particle position," Biophys. J., Vol. 67, pp. 1291-1300.

Kontoyannis, N. S. and Lanni, F., 1996, "Measured and computed point spread functions for an indirect water immersion objective used in three-dimensional fluorescence microscopy," Proc. Soc. Photo-optical Instr. Eng., Vol. 2655, pp. 34-42.

McNally, J. G., Preza, C., Conchello, J. A. and Thomas, L. J., 1994, "Artifacts in computational optical-sectioning microscopy," J. Opt. Soc. Am. A, Vol. 11, pp. 1056-1067.

Meinhart, C. D. and Wereley, S. T., 2003, "The theory of diffraction-limited resolution in microparticle image velocimetry," Meas. Sci. Technol., Vol. 14, pp. 1047-1053.

Meinhart, C. D., Wereley, S. T. and Gray, M. H. B., 2000, "Volume illumination for two-dimensional particle image velocimetry," Meas. Sci. Technol., Vol. 11, pp. 809-814.

Olsen, M. G. and Adrian, R. J., 2000, "Out-of-focus effects on particle image visibility and correlation in microscopic particle image velocimetry," Exp. Fluids, Suppl., S166-S174.

Park, J. S., Choi, C. K., Kihm, K. D. and Allen, J. S., 2003, "Optically-sectioned PIV measurements using CLSM," ASME J. Heat Transfer, Vol. 125, pp. 541-542.

Richards, B. and Wolf, E., 1959, "Electromagnetic diffraction in optical systems II. Structure of the image field in an aplanatic system," Proc. R. Soc. A, Vol. 253, pp. 358-379.

Santiago, J. G., Wereley, S. T., Meinhart, C. D., Beebe, D. J. and Adrian, R. J., 1998, "A particle image velocimetry system for microfluidics," Exp. Fluids, Vol. 25, pp. 316-319.

Sheppard, C. J. R., 1988, "Aberrations in high aperture conventional and confocal imaging systems," Appl. Opt., Vol. 27, pp. 4782-4786.

Sheppard, C. J. R. and Gu, M., 1991, "Aberration compensation in confocal microscopy," Appl. Opt., Vol. 30, pp. 3563-3568.

Speidel, M., Jonas, A. and Florin, E. L., 2003, "Three-dimensional tracking of fluorescent nanoparticles with subnanometer precision by use of off-focus imaging," Optics Letters, Vol. 28, pp. 69-71.

Webb, R. H., 1996, "Confocal optical microscopy," Rep. Prog. Phys., Vol. 59, pp. 427-471.

Wilson, T., (edited by) 1990, *Confocal microscopy*, Academic Press, London.